PERGAMON International Journal of Engineering Science 38 (2000) 1699–1712

International Journal of Engineering Science

www.elsevier.com/locate/ijengsci

Thermal radiation and buoyancy effects on hydromagnetic flow over an accelerating permeable surface with heat source or sink

Ali J. Chamkha *

Department of Mechanical and Industrial Engineering, Kuwait University, P.O. Box 5969, 13060 Safat, Kuwait

Received 12 May 1999; accepted 4 October 1999

Abstract

Similarity equations governing steady hydromagnetic boundary-layer flow over an accelerating permeable surface in the presence of such effects as thermal radiation, thermal buoyancy, and heat generation or absorption effects are obtained. These equations are solved numerically by an implicit finite-difference method. Favorable comparisons with previously published work are obtained. The effects of the various parameters on the velocity and temperature profiles as well as the skin-friction coefficient and wall heat transfer are presented graphically and in tabulated form.

1. Introduction

Boundary-layer flow and heat transfer over a continuously stretched surface has received considerable attention in recent years. This stems from various possible engineering and metallurgical applications such as hot rolling, wire drawing, metal and plastic extrusion, continuous casting, glass fiber production, crystal growing, and paper production. The first studies of boundary-layer flow over a continuous impermeable surface moving at a constant speed was carried out by Sakiadis [1,2]. His results showed a quite different behavior from the classical Blasius problem due to entrainment of ambient fluid into the boundary layer. Tsou et al. [3] reported both analytical and experimental results for the flow and heat transfer aspects developed by a continuously moving surface. Erickson et al. [4] and Fox et al. [5] extended Sakiadis' problem

* Tel.: +965-571-2298; fax: +965-484-7131.
E-mail address: chamkha@kuc01.kuniv.edu (A.J. Chamkha).

0020-7225/00/$ - see front matter
PII: S0020-7225(99)00134-2

to include wall suction or blowing effects and investigated its effects on the heat and mass transfer in the boundary layer. Many investigators have considered the problem of a stretched surface moving with a linear velocity with the axial distance for various temperature boundary conditions (see, for instance, [6–10]). Gupta and Gupta [11] extended the work of Erikson et al. [4] for the case of linear velocity movement of the stretched surface. Chen and Char [12] investigated the effects of both variable surface temperature and heat flux on the heat transfer characteristics of a linearly stretched surface subject to wall suction or injection.

Hydromagnetic flows and heat transfer have become more important in recent years because of many important applications. For example, in many metallurgical processes which involve cooling of continuous strips or filaments, these elements are drawn through a quiescent fluid. During this process, these strips are sometimes stretched. The properties of the final product depend to a great extent on the rate of cooling. This rate of cooling has been proven to be controlled and, therefore, the quality of the final product by drawing such strips in an electrically conducting fluid subject to a magnetic field [10]. Many works have been reported on flow and heat transfer over a stretched surface in the presence of a magnetic field (see, for instance, [10,13–15]).

In certain situations, such as those dealing with chemical reactions and dissociating fluids, heat generation or absorption may become important. This can be accounted for by addition of a source or sink term which represents this effect in the energy equation. In addition, thermal radiation and buoyancy effects can become more pronounced in flow and heat transfer over a continuously stretched surface. Therefore, the purpose of this study is to consider thermal radiation and buoyancy effects on hydromagnetic flow over an accelerating permeable surface with heat generation or absorption.

2. Problem formulation

Consider steady, laminar, viscous boundary-layer flow over an accelerating semi-infinite vertical permeable surface. A uniform magnetic field is applied in the horizontal direction that is normal to the surface. The surface is assumed to be permeable so as to allow for possible wall fluid suction or injection. A temperature-dependent heat source (or sink) is assumed to be present in the flow and that thermal radiation and buoyancy effects are significant. All fluid properties are assumed to be constant except the density in the body force term of the balance of linear momentum. The magnetic Reynolds number is assumed to be small so that the induced magnetic field is neglected. No electric field is assumed to exist and both viscous and magnetic dissipations are neglected. Under these assumptions, along with the Boussinesq approximation, the boundary-layer equations for this problem can be written as

$$\frac{\partial u}{\partial x} + \frac{\partial v}{\partial y} = 0, \tag{1}$$

$$u\frac{\partial u}{\partial x} + v\frac{\partial u}{\partial y} = \nu\frac{\partial^2 u}{\partial y^2} + g\beta(T - T_\infty) - \frac{\sigma B_0^2}{\rho}u, \tag{2}$$

$$u\frac{\partial T}{\partial x}+v\frac{\partial T}{\partial y}=\alpha\frac{\partial^2 T}{\partial y^2}+\frac{\beta^* u}{\rho c_p}(T_\infty-T)+\frac{Q_0}{\rho c_p}(T-T_\infty)-\frac{1}{\rho c_p}\frac{\partial q_r}{\partial y}, \tag{3}$$

where x and y are the vertical and horizontal directions, respectively. u, v, and T are the fluid velocity components in the x and y directions and temperature, respectively ρ, ν, c_p, and α $(k/(\rho c_p))$ are the fluid density, kinematics viscosity, specific heat at constant pressure, and thermal diffusivity, respectively. k, β, σ, B_0, and g are the fluid thermal conductivity, volumetric expansion coefficient, electric conductivity, applied magnetic induction, and the gravitational acceleration, respectively. q_r and T_∞ are the thermal radiation and the free stream temperature. The terms $\beta^* u(T_\infty - T)$ and $Q_0(T - T_\infty)$ (with β^* and Q_0 being constants) both represent the heat generated or absorbed per unit volume. The first form was used recently by Acharya et al. [16] while the last form was used by Vajravelu and Nayfeh [17] and Chamkha [18]. The reason for retaining both forms in the present work will be explained at a subsequent stage in this work.

By using Rosselant approximation and following Raptis [19], the radiative heat flux q_r is given by

$$q_r=-\frac{4\sigma^*}{3k^*}\frac{\partial T^4}{\partial y}, \tag{4}$$

where σ^* is the Stefan–Boltzmann constant and k^* is the mean absorption coefficient.

Assuming that the temperature differences within the flow are sufficiently small so that T^4 can be expanded in Taylor series about the free stream temperature T_∞ to yield

$$T^4 \cong 4T_\infty^3 T - 3T_\infty^4, \tag{5}$$

where the higher-order terms of the expansion are neglected.

By employing Eqs. (4) and (5), Eq. (2) becomes

$$u\frac{\partial T}{\partial x}+v\frac{\partial T}{\partial y}=\alpha\frac{\partial^2 T}{\partial y^2}+\frac{\beta^* u}{\rho c_p}(T_\infty-T)+\frac{Q_0}{\rho c_p}(T-T_\infty)+\frac{16\sigma^* T_\infty^3}{3\rho c_p k^*}\frac{\partial^2 T}{\partial y^2}. \tag{6}$$

The boundary conditions for this problem can be written as

$$\begin{aligned} &u(x,0)=ax, \quad v(x,0)=v_{\mathrm{w}},\\ &T(x,0)=T_{\mathrm{w}}(x)=T_\infty+A_0x,\\ &u(x,\infty)=0, \quad T(x,\infty)=T_\infty, \end{aligned} \tag{7}$$

where a is the stretching rate (a constant), v_{w} is the wall suction ($v_{\mathrm{w}} < 0$) or injection ($v_{\mathrm{w}} > 0$) velocity, and $T_{\mathrm{w}}(x)$ is the wall temperature.

Using the usual definition for the stream function ψ such that $u = \partial\psi/\partial y$, $v = -\partial\psi/\partial x$ and substituting the following similarity transformation

$$\psi=(\nu a)^{1/2}xf(\eta), \quad \eta=\left(\frac{a}{\nu}\right)^{1/2}y, \quad \theta(\eta)=\frac{T-T_\infty}{T_w-T_\infty} \tag{8}$$

into Eqs. (1)–(3) yields

$$f''' + ff'' - (f')^2 - M^2 f' + Gr\,\theta = 0, \tag{9}$$

$$\frac{(N_R + 1)}{Pr}\theta'' + f\theta' - (1 + \delta_x)f'\theta + \Delta\theta = 0, \tag{10}$$

where

$$M = \left(\frac{\sigma}{\rho a}\right)^{1/2} B_0, \quad Gr = \frac{g\beta(T_w - T_\infty)}{a^2 x}, \quad Pr = \frac{\nu}{\alpha},$$
$$N_R = \frac{16\sigma^* T_\infty^3}{3k^* k}, \quad \delta_x = \frac{\beta^* x}{\rho c_p}, \quad \Delta = \frac{Q_0}{\rho c_p a}, \tag{11}$$

are the Hartmann number, Grashof number, Prandtl number, thermal radiation parameter and heat generation or absorption coefficients, respectively. It is seen from Eq. (11) that using a heat generation or absorption effect of the form $\beta^* u(T_\infty - T)$ produces a locally similar set of equations since δ_x depends on x. However, by employing the form $Q_0(T - T_\infty)$ yields self-similar equations everywhere along the surface. Since one of the objectives of this work is to obtain similarity equations, the second form for the heat generation or absorption effect is employed. Also, the first form is kept in the formulation for merely comparison purposes with [16]. It should be noted here that positive values of Δ indicate heat generation while negative values of Δ indicate heat absorption.

The transformed boundary conditions become

$$f'(0) = 1, \quad f(0) = -f_0, \quad \theta(0) = 1,$$
$$f'(\infty) = 0, \quad \theta(\infty) = 0, \tag{12}$$

where $f_0 = v_w/(a\nu)^{1/2}$ is the wall mass transfer coefficient such that $f_0 < 0$ indicates wall suction and $f_0 > 0$ corresponds to wall blowing conditions.

The skin-friction coefficient and the wall heat transfer are important physical parameters for this flow and heat transfer situation. These parameters can be defined as follows:

$$C_f = \frac{\tau_w}{\mu(a/\nu)^{1/2} a x} = \frac{\mu(\partial u/\partial y)(x,0)}{\mu(a/\nu)^{1/2} a x} = f''(0), \tag{13}$$

$$Q = \frac{q_w}{k(a/\nu)^{1/2}(T_w - T_\infty)} = \frac{-k(\partial T/\partial y)(x,0)}{k(a/\nu)^{1/2}(T_w - T_\infty)} = -\theta'(0), \tag{14}$$

where τ_w and q_w are the dimensional shear stress and heat transfer at the accelerating surface. It is seen that C_f and Q are directly proportional to the wall velocity and temperature gradients, respectively.

In the absence of buoyancy effects ($Gr = 0$), the flow problem is uncoupled from the thermal problem. For this situation, the flow equation (9) can be solved in closed form subject to the flow boundary conditions in Eq. (12). This closed-form solution was reported previously by Chakrabarti and Gupta [20] and can be written as

$$f(\eta) = \alpha_1 + \alpha_2 \exp(-\alpha_3 \eta), \tag{15}$$

where α_1, α_2 and $\alpha_3 (> 0)$ are constants given by

$$\alpha_1 = \frac{1}{2(1+M^2)} \left\{ [f_0^2 + 4(1+M^2)]^{1/2} - f_0(1+2M^2) \right\}, \tag{16}$$

$$\alpha_2 = \frac{2}{f_0 - [f_0^2 + 4(1+M^2)]^{1/2}}, \qquad \alpha_3 = \frac{1}{2}\left[\alpha_1 + (\alpha_1^2 + 4M^2)^{1/2}\right]. \tag{17}$$

The skin-friction coefficient for this case becomes

$$C_{\mathrm{f}} = f''(0) = \alpha_2 \alpha_3^2. \tag{18}$$

In the limit as $M \to 0$ (no magnetic field), the solutions for $f(\eta)$ and $f''(0)$ become

$$f(\eta) = m - \frac{1}{m}\exp(-m\eta), \qquad f''(0) = -m \tag{19}$$

such that

$$f_0 = -\left(m - \frac{1}{m}\right). \tag{20}$$

In addition, for the case of impermeable wall ($f_0 = 0$) the solutions for $f(\eta)$ and $f''(0)$ become

$$f(\eta) = 1 - \exp(-\eta), \qquad f''(0) = -1, \tag{21}$$

which are consistent with those of Crane [6].

3. Numerical method and validation

In the presence of buoyancy effects ($Gr \neq 0$), the flow and thermal problems are coupled and must be solved simultaneously. An analytical solution of Eqs. (9) and (10) subject to Eq. (12) appears to be impossible. Therefore, a numerical solution must be obtained. The type of Eqs. (9) and (10) is suitable for solution by the fourth-order Runge–Kutta method or by the implicit finite-difference method discussed by Blottner [21]. Since the finite-difference method is more accurate and more flexible in setting the limiting condition far from the surface than the Runge–Kutta method, it is adopted in the present work.

Eqs. (9) and (10) are discretized using three-point central difference formulae with f' being replaced by another variable V. The equation $f' = V$ is discretized using the trapezoidal rule. The η direction is divided into 196 nodal points and a variable step size is used to account for the sharp changes in the variables in the immediate vicinity of the surface where viscous effects dominate. The initial step size used is $\Delta\eta_1 = 0.001$ and the growth factor $K = 1.03$ such that $\Delta\eta_n = K\,\Delta\eta_{n-1}$ (where the subscript n is the number of nodes − 1). The ordinary differential equations are then converted into linear algebraic difference equations that are solved by the Thomas algorithm discussed by Blottner [21]. Iteration is employed to deal with the nonlinear nature of the original governing equations. The convergence criterion employed in this work was based on the relative difference between the current and the previous iterations. When this difference or error reached 10^{-5}, the solution was assumed converged and the iteration process was terminated.

Table 1 presents a comparison of the wall heat transfer $Q = -\theta'(0)$ for various values of the suction or injection parameter f_0 and the heat generation or absorption parameter δ_x with those reported previously by Acharya et al. [16]. It is seen from this table that excellent agreement between the results exists. In addition, the closed-form solution reported earlier by Crane [6] (Eq. (21)) is also compared favorably with the numerical result for $Gr = 0$ reported in Fig. 1. These favorable comparisons lend confidence in the accuracy of the numerical procedure.

Table 1
Comparison of wall temperature gradient ($-\theta'(0)$) with Acharya et al. [16][a]

	$f_0 = 0.45$ $\delta_x = 0.5$	$f_0 = 0.45$ $\delta_x = 1.0$	$f_0 = 0$ $\delta_x = 0.5$	$f_0 = 0$ $\delta_x = 1.0$	$f_0 = -1.5$ $\delta_x = 0.5$	$f_0 = -1.5$ $\delta_x = 1.0$
Present work	0.82397	0.96191	0.94769	1.07996	1.57077	1.66184
Acharya et al. [16]	0.82250	0.96180	0.94620	1.07890	1.56960	1.66030

[a] $Gr = 0$, $M = 0$, $N_R = 0$, $Pr = 0.71$ and $\Delta = 0$.

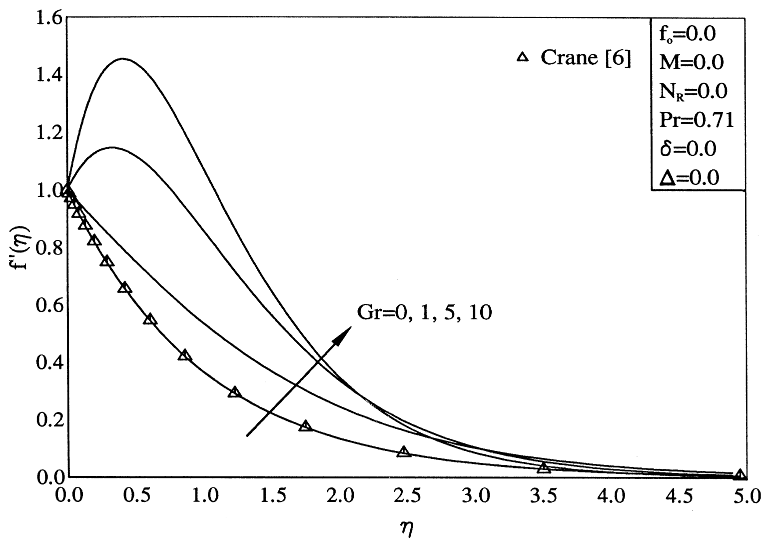

Fig. 1. Effects of Gr on velocity profiles.

4. Results and discussion

Figs. 1 and 2 present typical velocity and temperature profiles in the boundary layer adjacent to the surface for various values of the Grashof number *Gr*, respectively. All of the parameters for the other effects are set to zero in order to study the influence of a single effect at a time. Increases in the values of *Gr* have the tendency to induce more flow in the boundary layer due to the effect of the thermal buoyancy. For small buoyancy effects ($Gr = 1$), the maximum flow velocity occurs at the surface. However, as the buoyancy effects get relatively large, a distinctive peak in the velocity profile occurs in the fluid adjacent to the wall and this peak becomes more distinctive as *Gr* increases further. Along with this flow behavior, the thermal boundary layer reduces as *Gr* increases causing the fluid temperature to reduce at every point other than that of the wall. These flow and thermal behaviors are depicted by the respective increases and decreases in the velocity and temperature fields as *Gr* increases shown in Figs. 1 and 2.

Figs. 3 and 4 illustrate the influence of the Hartmann number *M* on the velocity and temperature profiles in the boundary layer, respectively. Application of a transverse magnetic field to an electrically conducting fluid gives rise to a resistive-type force called the Lorentz force. This force has the tendency to slow down the motion of the fluid in the boundary layer and to increase its temperature. Also, the effects on the flow and thermal fields become more so as the strength of the magnetic field increases. This is obvious from the decreases in the velocity profiles and the increases in the temperature profiles presented in Figs. 3 and 4.

The effects of the thermal radiation parameter N_R on the velocity and temperature profiles in the boundary layer are illustrated in Figs. 5 and 6, respectively. Increasing the thermal radiation parameter N_R produces significant increases in the thermal condition of the fluid and its thermal boundary layer. Through the buoyancy effect, this increase in the fluid temperature induces more flow in the boundary layer causing the velocity of the fluid there to increase. In addition,

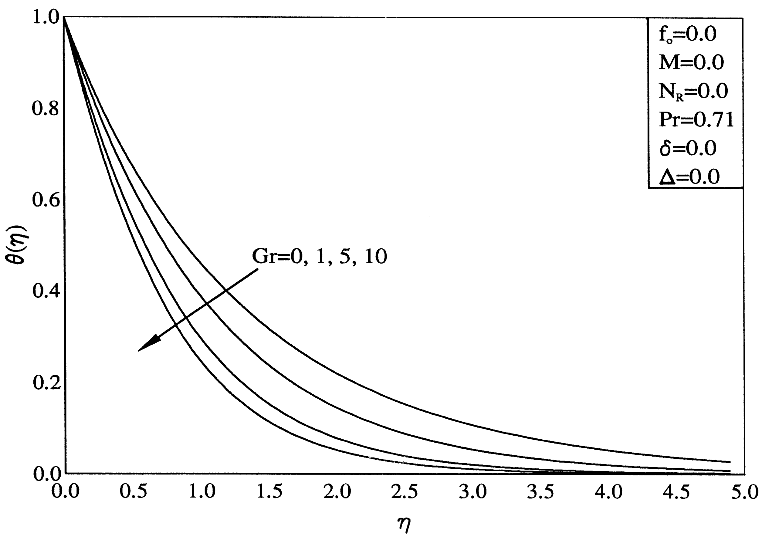

Fig. 2. Effects of *Gr* on temperature profiles.

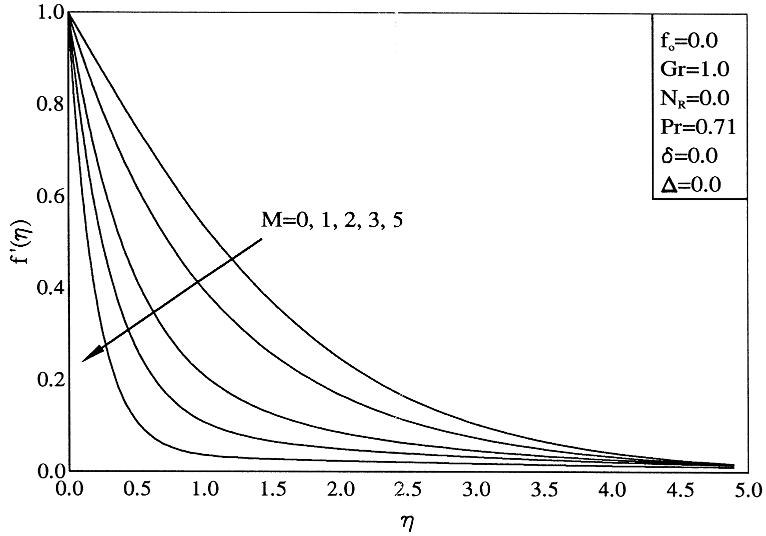

Fig. 3. Effects of M on velocity profiles.

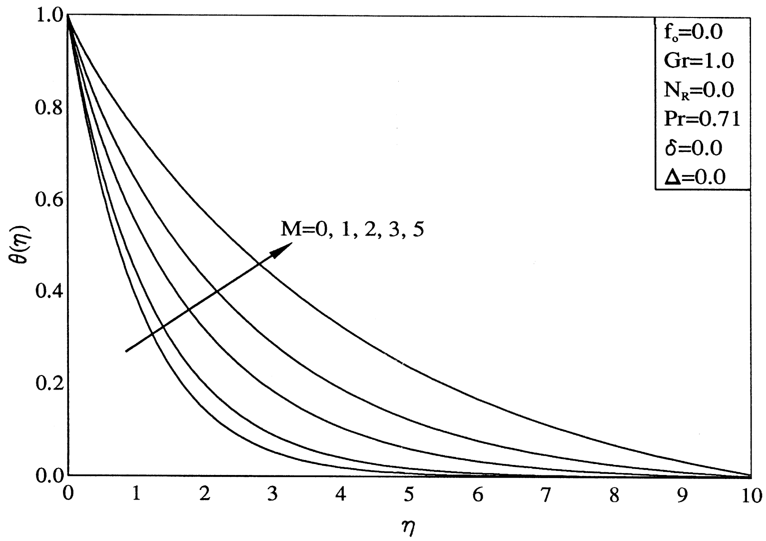

Fig. 4. Effects of M on temperature profiles.

the hydrodynamic boundary layer thickness increases as a result of increasing N_R. These behaviors are clearly shown in Figs. 5 and 6.

Figs. 7 and 8 depict the influence of the suction/injection parameter f_0 on the velocity and temperature profiles in the boundary layer, respectively. It is known that imposition of wall fluid suction reduces both the hydrodynamic and thermal boundary layers which indicates reduction in both the fluid velocity and temperature profiles. However, the exact opposite behavior is produced by imposition of wall fluid blowing or injection. These behaviors are clear from Figs. 7 and 8.

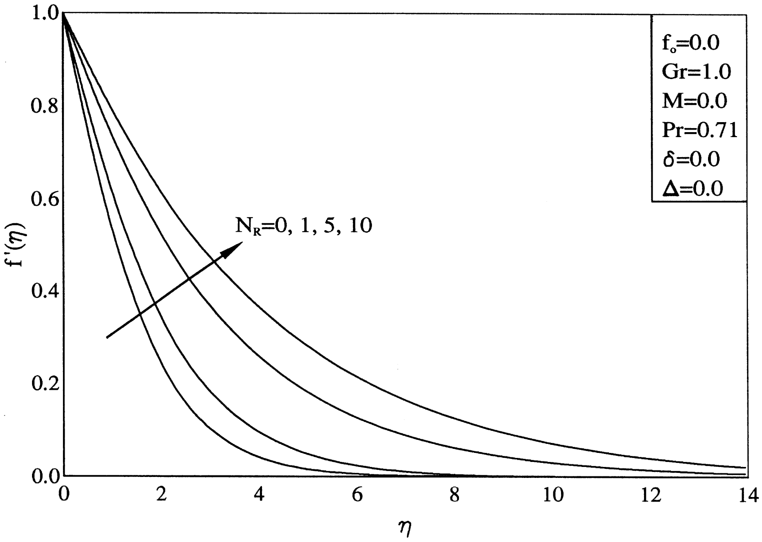

Fig. 5. Effects of N_R on velocity profiles.

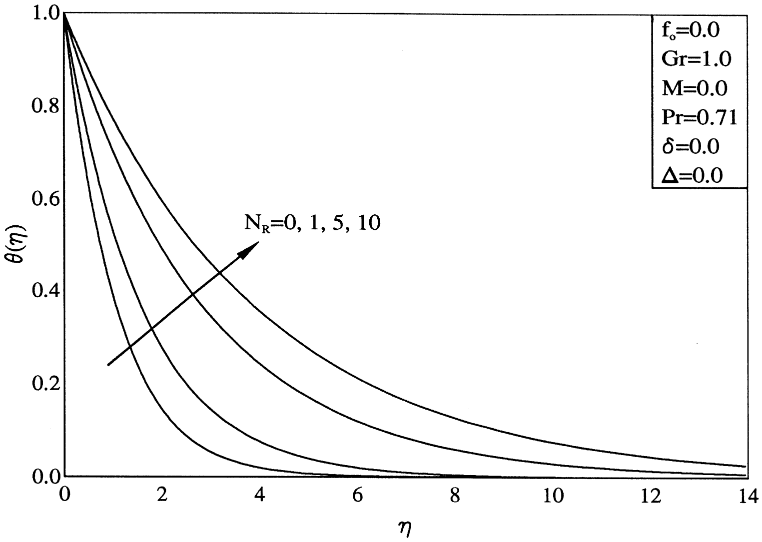

Fig. 6. Effects of N_R on temperature profiles.

The influence of the presence of a heat source ($\Delta > 0$) or a heat sink ($\Delta < 0$) in the boundary layer on the velocity and temperature fields is presented in Figs. 9 and 10, respectively. The presence of a heat source in the boundary layer generates energy which causes the temperature of the fluid to increase. This increase in temperature produces an increase in the flow field due to the buoyancy effect. On the other hand, the presence of a heat sink in the boundary layer absorbs energy which causes the temperature of the fluid to decrease. This decrease in the fluid temper-

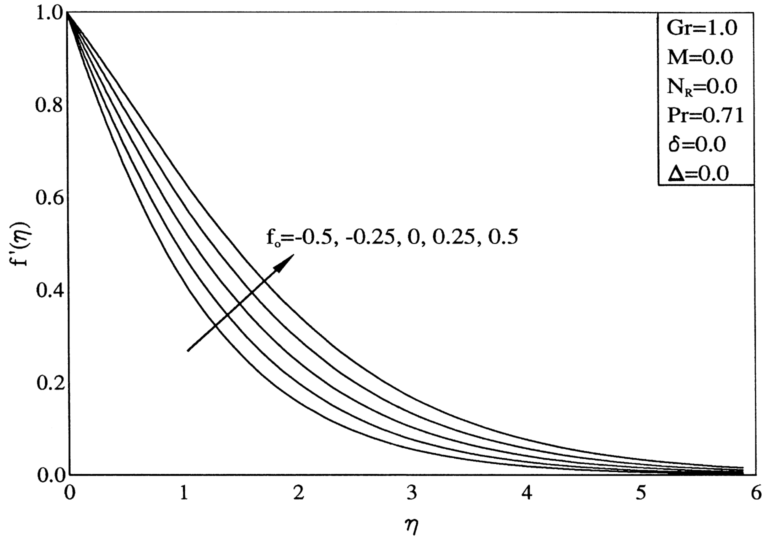

Fig. 7. Effects of f_0 on velocity profiles.

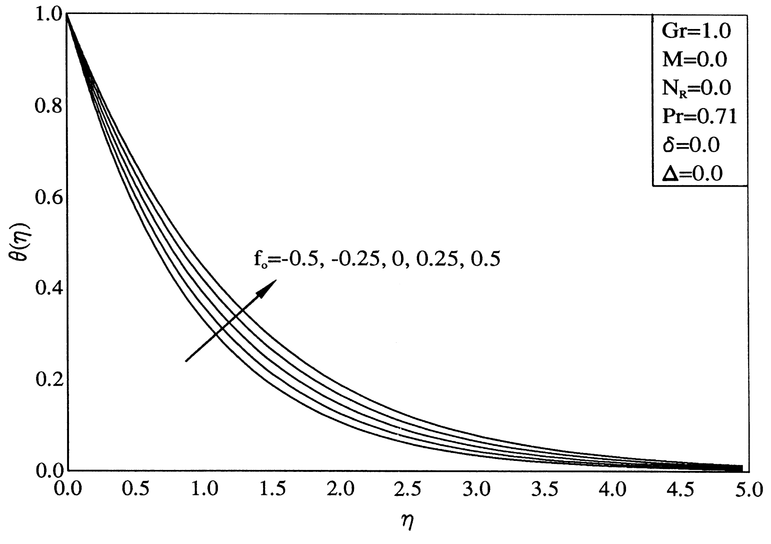

Fig. 8. Effects of f_0 on temperature profiles.

ature causes a reduction in the flow velocity in the boundary layer as a result of the buoyancy effect which couples the flow and thermal problems. These behaviors are depicted in Figs. 9 and 10.

Tables 2 and 3 illustrate the effects of f_0, M, and N_R on both the wall velocity and temperature gradients $-f''(0)$ and $-\theta'(0)$, respectively. As mentioned before increasing the value of the suction/injection parameter f_0 causes both the hydrodynamic and thermal boundary layers to

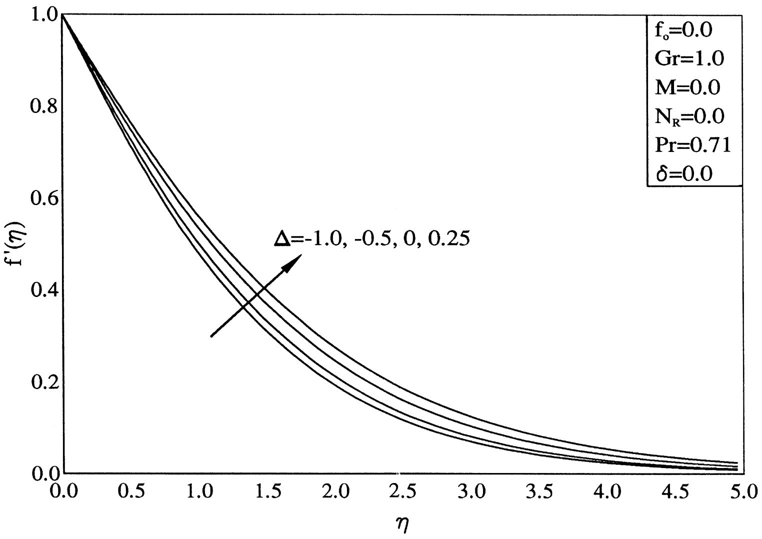

Fig. 9. Effects of Δ on velocity profiles.

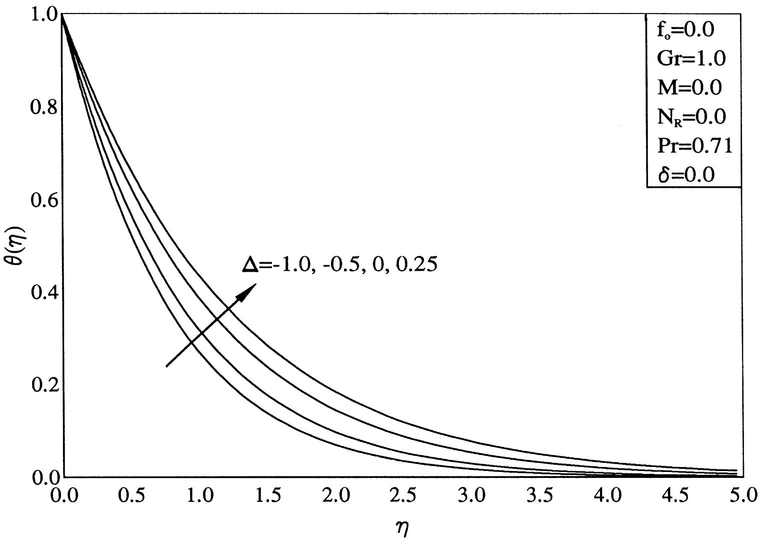

Fig. 10. Effects of Δ on temperature profiles.

increase causing the wall gradients of both the velocity and temperature profiles to decrease. This is consistent with Figs. 7 and 8 and is depicted in the decreases of $-f''(0)$ and $-\theta'(0)$ as f_0 increases shown in Tables 2 and 3. Similarly, Figs. 5 and 6 show that as the thermal radiation parameter N_R increases, the wall gradients of both the velocity and temperature profiles decrease. However, while the wall velocity gradient $-f''(0)$ increases as the Hartmann Number M increases, the wall heat transfer $-\theta'(0)$ decreases as predicted in Tables 2 and 3.

Table 2
Wall velocity gradient $(-f''(0))$ for various f_0, M and N_R values[a]

M	$f_0 = -0.5$ $N_R = 0$	$f_0 = 0$ $N_R = 0$	$f_0 = 0.5$ $N_R = 0$	$f_0 = -0.5$ $N_R = 5.0$	$f_0 = 0$ $N_R = 5.0$	$f_0 = 0.5$ $N_R = 5.0$
0	0.77130	0.51157	0.32742	0.40921	0.27405	0.17859
5	5.17166	4.91476	4.67416	5.15463	4.90735	4.67123

[a] $Gr = 1.0$, $Pr = 0.71$, $\delta_x = 0$ and $\Delta = 0$.

Table 3
Wall temperature gradient $(-\theta'(0))$ for various f_0, M and N_R values[a]

M	$f_0 = -0.5$ $N_R = 0$	$f_0 = 0$ $N_R = 0$	$f_0 = 0.5$ $N_R = 0$	$f_0 = -0.5$ $N_R = 5.0$	$f_0 = 0$ $N_R = 5.0$	$f_0 = 0.5$ $N_R = 5.0$
0	1.08377	0.90521	0.75443	0.37375	0.35239	0.33215
5	0.63779	0.36508	0.21762	0.14673	0.11218	0.08478

[a] $Gr = 1.0$, $Pr = 0.71$, $\delta_x = 0$ and $\Delta = 0$.

Tables 4 and 5 depict the effects of the buoyancy parameter or Grashof number Gr and the heat generation or absorption parameter Δ on $-f''(0)$ and $-\theta'(0)$, respectively, it is seen earlier from Fig. 1 that for $Gr = 5$ a distinctive peak in the velocity profile exists. This causes its wall slope to become positive which means $-f''(0)$ is negative. This explains the decrease in $-f''(0)$ as Gr increases. On the other hand, Fig. 2 shows that $-\theta'(0)$ increases as Gr increases. This is consistent with Table 5. Increasing the value of the heat generation or absorption parameter Δ is predicted to

Table 4
Wall velocity gradient $(-f''(0))$ for various Gr and Δ values[a]

Gr	$\Delta = -1.0$	$\Delta = 0$	$\Delta = 0.5$
0	1.00241	1.00241	1.00241
5	−0.80542	−0.99399	−1.12152

[a] $f_0 = 0$, $M = 0$, $N_R = 0$, $Pr = 0.71$ and $\delta_x = 0$.

Table 5
Wall temperature gradient $(-\theta'(0))$ for various Gr and Δ values[a]

Gr	$\Delta = -1.0$	$\Delta = 0$	$\Delta = 0.5$
0	1.21338	0.80405	0.57944
5	1.34695	1.06986	0.90408

[a] $f_0 = 0$, $M = 0$, $N_R = 0$, $Pr = 0.71$ and $\delta_x = 0$.

cause no effect on $-f''(0)$ for $Gr=0$ since the flow and thermal problems are uncoupled and to decrease it for $Gr=5$. The wall heat transfer $-\theta'(0)$ is also predicted to decrease as Δ increases. These behaviors are clearly displayed in Tables 4 and 5.

5. Conclusion

The problem considered in this work was that of steady, hydromagnetic boundary-layer flow over an accelerating semi-infinite porous surface in the presence of thermal radiation, buoyancy and heat generation or absorption. A similarity transformation was employed to change the governing partial differential equations into ordinary ones. These equations were solved numerically by the finite-difference methodology. The obtained results were compared with previously published work and were found to be in excellent agreement. It was found that owing to the presence of thermal radiation, positive wall mass transfer, magnetic field, or heat generation, the wall heat transfer decreased. However, the wall heat transfer increased due to the presence of the thermal buoyancy effect. It is hoped that the solutions presented in this work with the various investigated effects would be useful for validation of future work on flow and heat transfer on a continuously stretched surface.

References

[1] B.C. Sakiadis, Boundary-layer behavior on continuous solid surfaces: I. Boundary-layer equations for two-dimensional and axisymmetric flow, AIChE J. 7 (1961) 26–28.

[2] B.C. Sakiadis, Boundary-layer behavior on continuous solid surfaces: II. The boundary layer on a continuous flat surface, AIChE J. 7 (1961) 221–225.

[3] F.K. Tsou, E.M. Sparrow, R.J. Goldstein, Flow and heat transfer in the boundary layer on a continuous moving surface, Int. J. Heat Mass Transfer 10 (1967) 219–235.

[4] L.E. Erickson, L.T. Fan, V.G. Fox, Heat and mass transfer on a moving continuous flat plate with suction or injection, Ind. Eng. Chem. 5 (1966) 19–25.

[5] V.G. Fox, L.E. Erickson, L.T. Fan, Methods for solving the boundary layer equations for moving continuous flat surfaces with suction and injection, AIChE J. 14 (1968) 726–736.

[6] L.J. Crane, Flow past a stretching plane, Z. Angew. Math. Phys. 21 (1970) 645–647.

[7] J. Vleggar, Laminar boundary-layer behavior on continuous accelerating surfaces, Chem. Eng. Sci. 32 (1977) 1517–1525.

[8] V.M. Soundalgekar, T.V. Ramana Murty, Heat transfer past a continuous moving plate with variable temperature, WarmeUnd Stoffubertragung 14 (1980) 91–93.

[9] L.G. Grubka, K.M. Bobba, Heat transfer characteristics of a continuous stretching surface with variable temperature, J. Heat Transfer 107 (1985) 248–250.

[10] K. Vajravelu, A. Hadjinicolaou, Convective heat transfer in an electrically conducting fluid at a stretching surface with uniform free stream, Int. J. Eng. Sci. 35 (1997) 1237–1244.

[11] P.S. Gupta, A.S. Gupta, Heat and mass transfer on a stretching sheet with suction or blowing, Can. J. Chem. Eng. 55 (1977) 744–746.

[12] C.K. Chen, M. Char, Heat transfer of a continuous stretching surface with suction or blowing, J. Math. Anal. Appl. 135 (1988) 568–580.

[13] T.C. Chiam, Hydromagnetic flow over a surface stretching with a power-law velocity, Int. J. Eng. Sci. 33 (1995) 429–435.

[14] I. Pop, T.Y. Na, A note on MHD flow over a stretching permeable surface, Mech. Res. Commun. 25 (1998) 263–269.
[15] A.J. Chamkha, Hydromagnetic three-dimensional free convection on a vertical stretching surface with heat generation or absorption, Int. J. Heat Fluid Flow, in press.
[16] M. Acharya, L.P. Singh, G.C. Dash, Heat and mass transfer over an accelerating surface with heat source in presence of suction and blowing, Int. J. Eng. Sci. 37 (1999) 189–211.
[17] K. Vajravelu, J. Nayfeh, Hydromagnetic convection at a cone and a wedge, Int. Commun. Heat Mass Transfer 19 (1992) 701–710.
[18] A.J. Chamkha, Non-Darcy hydromagnetic free convection from a cone and a wedge in porous media, Int. Commun. Heat Mass Transfer 23 (1996) 875–887.
[19] A. Raptis, Flow of a micropolar fluid past a continuously moving plate by the presence of radiation, Int. J. Heat Mass Transfer 41 (1998) 2865–2866.
[20] A. Chakrabarti, A.S. Gupta, Hydromagnetic flow and heat transfer over a stretching sheet, Q. Appl. Math. 37 (1979) 73–78.
[21] F.G. Blottner, Finite-difference methods of solution of the boundary-layer equations, AIAA J. 8 (1970) 193–205.